The University of Reading School of Mathematics, Meteorology & Physics

Moving Mesh Methods for Semi-Linear Problems

by

Matthew Paul Edgington

August 2011

Abstract

In this dissertation we examine the application of moving mesh methods to a number of semi-linear partial di erential equations (PDEs). In particular we apply moving mesh methods that are based on the principle of conservation of certain quantities. The PDEs we consider are the Fisher's equation, Non-linear Schredinger equation and the Cahn-Allen equation. We begin with some examples of PDEs that exhibit blow-up behaviour, that is, they have a solution that becomes in nite within a nite time, and then investigate some applications to other problems not displaying blow-up behaviour. The main aim of this dissertation is to examine the e ects of using these conservative moving mesh methods on the capture of the solutions obtained for the speci c PDEs considered and then to discuss the results obtained.

Acknowledgements

I would like to begin by acknowledging Professor Mike Baines for his help and support during the course of this dissertation. In particular I would like to thank him for always being available to help and for being an endless source of information and guidance. All of this on top of being a genuinely nice person.

I would also like to thank all of the academic sta in both the mathematics and meteorology departments who make this course what it is. A special mention must also go to Dr. Peter Sweby for his excellent organisation of the Mathematical and Numerical Modelling of the Atmosphere and Oceans MSc course.

A huge debt of gratitude is also owed to everyone who encouraged me to return to university and pursue my interests.

Finally, I must thank the Natural Environment Research Council (NERC) for their nancial support, without which I would not have been able to further my education in this way.

Declaration

con rm that this is my own work and the use of all material from other source
nas been properly and fully acknowledged.
Signed Date

Contents

1	Intr	roduction	1
	1 1	Why do we use moving mesh methods?	

3	Alternative `Fisher Type' Equations 25					
	3.1	Introd	luction to `Fisher Type' Equations	25		
	3.2	Choos	ing an Appropriate Monitor Function	26		
	3.3	`Tradi	tional' Fisher's Equation	28		
		3.3.1	Problem Formation	28		
	3.4	Metho	od for the `Traditional' Fisher's Equation	29		
		3.4.1	Generation of Nodal Velocities	29		
		3.4.2	New Mesh and Arc-Length Creation	31		
		3.4.3	Recovery of New Approximations	31		
	3.5	Cahn-	Allen Equation	33		
		3.5.1	Problem Formation	33		
	3.6 Method for the Cahn-Allen Equation					
	3.7	Nume	rical Results	34		
		3.7.1	Results for the `Traditional' Fisher's Equation	34		
		3.7.2	Results for the Cahn-Allen Equation	36		
	3.8	Summ	ary of Other `Fisher Type' Equations	37		
4	The	Nonli	inear Schredinger Equation	38		
	4.1	Introd	uction to the Nonlinear Schredinger Equation	38		
	4.2	Proble	em Formation	39		
	4.3	`Mass'	Conservative Method for the Nonlinear Schredinger Equa-			
		tion		40		
		4.3.1	Analysis of Properties	40		
		4.3.2	Calculating Conserved Quantities	44		
		4.3.3	Generation of New Meshes	44		
		4.3.4	Recovering New Approximations of and			

	4.5	Area Conservative Method for Non-linear Schrødinger Equation . 51						
		4.5.1 Generation of Node Velocities 5						
		4.5.2 Generating New Meshes and Total Areas 54						
		4.5.3 Recovery of New Approximations 54						
	4.6	Results for the Area Conservation Method for the Nonlinear Schredinge						
		Equation						
	4.7	Nonlinear Schredinger Equation Summary						
5	Disc	ussion of Project 58						
	5.1	Summary						
	5.2	Conclusions						
	53	Further Work 66						

List of Figures

1.1	An example of a typical blow-up solution pro le	3
1.2	An example of a typical phase eld problem solution	4
2.1	Solution of Fisher's equation for 165 time steps using an explicit	
	method	8
2.2	Solution of Fisher's equation for 5 time steps using a semi-implicit	
	method	9
2.3	Solution of Fisher's equation (with $p=2$) at the $\ $ nal time step $\ $.	16
2.4	Development of time-steps	17
2.5	Mesh evolution	18
2.6	Demonstration of the method of linear extrapolation of velocities	19
2.7	Comparison of results obtained using a xed and a moving bound-	
	ary node method	21
2.8	Solution of Fisher's equation (with $p=3$) at the $\ $ nal time step $\ $.	23
2.9	Mesh evolution in Fisher's equation with $p = 3 \dots \dots \dots$	24
3.1	Solution obtained for the `Traditional' Fisher's equation	35
3.2	Mesh Evolution for the `Traditional' Fisher's equation	35
3.3	Solution obtained for the Cahn-Allen equation	36
3.4	Mesh Evolution for the Cahn-Allen equation	37
4.1	Demonstration of the method of Lagrange polynomials to extrap-	
	olate solutions	17

4.2	Real part of the `i	mass'	cons	ervativ	ve so	olutio	n of	the	Non	line	ar	
	Schrodinger Equati	ion .										49

List of Tables

2.1	Cases considered for the number of nodes in $x \ge [0;1]$ and t_0 in	
	Fisher's equation	15
2.2	Number of nodes and initial time steps used for comparison of	15

Chapter 1

Introduction

1.1 Why do we use moving mesh methods?

of nodes which are redistributed at each time step in order to track the blow-up behaviour as it develops. The main advantages of this type of method are that it allows computations to be carried out all the way up to the blow-up time and also it is not computationally expensive to do so. There is however a weakness in that as the nodes track the blow-up behaviour (i.e. they move towards the blow-up point) the nodes away from the blow-up point become more sparsely distributed meaning that the solution in these areas may be poorly represented.

In this project we shall focus our attention on r

1.3 What is a phase eld problem?

According to Westwood [2], phase eld models are used to represent situations whereby a sharp interface is represented by very thin transition layers so that the phase eld varies continuously over these transition layers, and yet remains uniform over the bulk phases.

Zhang and Du [5] state that one of the most important challenges of modeling this type of problem is to suitably resolve the thin interfacial layer. In this small layer the solution will remain smooth, but develop a large spatial gradient. Zhang and Du [5] go on to explain that cases where such layers move over time may be used to model dynamically evolving fronts.

The literature on this type of problem clearly shows somewhat of a typical solution which has a very speci c form. This is that in a case with two phases P_1 and P_2 , there will be a smooth curve from each phase into a linear slope between them. An example of such a solution can be seen in Figure (1.2).

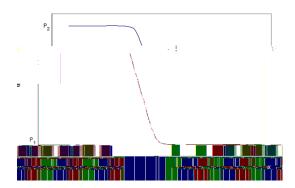


Figure 1.2: An example of a typical phase eld problem solution

Chapter 2

Blow-Up in Fisher's

Equation

Our investigation into the application of moving mesh methods in the solution of various PDEs begins with the examination of Fisher's equation and this is a common starting point when considering blow-up problems.

2.1 Introduction to Fisher's Equation

Fisher's equation is the standard one-dimensional heat equation with an extra source term and is given by

$$u_t = u_{xx} + u^p; \quad (p > 1):$$
 (2.1)

Fisher's equation has applications in many areas of science as described in [3], [6] and [7]. Budd et al. [3] state that the equation is used as a representation of the temperature in a reacting or combusting medium, whilst Braun and Kluwick [6] and Kluwick et al. [7] explain a use of Fisher's equation in the representation of various processes involved in laminar boundary layer separation, which is a key research area within meteorological science.

Fisher's equation is an example of a typical blow-up problem in so much as the solution can exhibit blow-up at a single blow-up point, denoted x, and this will occur within a nite blow-up time, T. Budd et al. [3] describe this by saying that for some blow-up time T < 1, as $t \nmid T$ we have

$$u(x;t) / 1$$
 and $u(x;t) / u(x;T) < 1$; if $x \in x$:

2.2 Problem Formation

In examining Fisher's equation we will consider two different cases which are related to the power of the blow-up term. We begin by considering the case in [3] where p=2 and we will then go on to look at the case where p=3, i.e. we will examine

$$U_t = U_{xx} + U^2 \tag{2.2}$$

and

$$U_t = U_{XX} + U^3 \tag{2.3}$$

in $x \ge [0;1]$. Throughout our investigation into Fisher's equation we will use Dirichlet boundary conditions of the form

$$u(0; t) = u(1; t) = 0$$
:

According to Budd et al. [3] our choice of initial condition must be large enough to ensure that blow-up will occur and also must be chosen such that our problem will display blow-up at a single blow-up point (in this case x=0.5). With these considerations in mind we take our initial condition to be that given in [8], i.e.

$$u(x;0) = 20 \sin(x)$$
:

2.3 Fisher's Equation on a Fixed Mesh

In order to demonstrate the need for moving mesh methods we rst consider Fisher's equation as in Equation (2.2), as discussed previously and examine two di erent solution methods which both utilise a xed mesh. The two xed mesh methods we consider are very simple explicit and semi-implicit solution methods. We will then discuss the results obtained and demonstrate the need for a moving mesh method for solving blow-up problems.

2.3.1 Explicit Method

One of the simplest methods which can be used to solve Fisher's equation numerically is to utilise nite di erence methods applied on a xed mesh (i.e. a mesh made of static nodes). This will give us some insight into the blow-up solution of Fisher's equation and act as a benchmark against which to compare results.

Using a forward di erence in time and a central di erence in space we may discretise Fisher's equation to obtain

$$u_j^{n+1}$$
 u_j^n

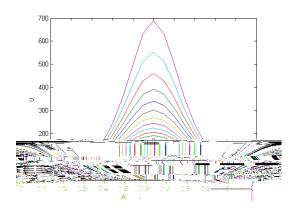


Figure 2.1: Solution of Fisher's equation for 165 time steps using an explicit method

We can clearly see that in this case we have a blow-up point located at x=0.5. It is also the case that as our blow-up peak grows taller and narrower, we can see that our xed mesh method fails to resolve the solution and with this being the case, under a xed mesh method we would need to add extra nodes into our mesh in order to add extra resolution to the solution.

Another common issue with using a xed mesh to tackle a blow-up problem is that the blow up point, x, may not actually be located at one of the nodes leading to an even greater failure of the xed mesh method to resolve the solution of the blow-up problem.

2.3.2 Semi-Implicit Method

r 9 \$\forall n \tag{1.423} 366693.9[3937579]5

The stability condition referred to in Section (2.3.1) is the main weakness associated with using an explicit method in order to solve problems and so we now extend our investigation into xed mesh solutions of blow-up problems by considering a semi-implicit solution method. As in Section (2.3.1) we begin by discretising Fisher's equation, however in this case we discretise our spatial derivative at the forward time which gives

$$U_j^{n+1} \quad U_j^r$$

and this rearranges to

$$U_j^{n+1}$$
 U_{j+1}^{n+1} $2U_j^{n+1} + U_{j-1}^{n+1} = U_j^n + t U_j^{n-2};$

where again = t

here is the form of r-re nement whereby we aim to conserve the fractional area under the curve as our solution evolves.

2.4.1 Generating Node Velocities

In order to guide the movement of the nodes making up our mesh we consider a velocity-based approach whereby each node is assigned a velocity with which it will move towards the blow-up point. This is recalculated at each time step and a new mesh is created. The velocity with which the nodes are allowed to move is calculated in such a way that the fractional area under the solution curve is conserved at each time step.

We begin by splitting our domain $x \ge [0;1]$ into two halves since we know the solution is symmetric. The domain now becomes $x \ge [0:5;1]$, which is divided into N equally sized intervals which shall be denoted by $(x_{j-1}(t);x_{j}(t))$, for j=1;2

into which we may substitute (2.2) in place of u_t , giving

$$\begin{array}{rcl}
 & & Z_{1} \\
- & = & u_{xx} + u^{2} dx \\
& & 0.5 & Z_{1} \\
& = & [u_{x}]_{0.5}^{1} + u^{2} dx :
\end{array} (2.7)$$

In the method of conservation we hold the fractional area of the regions under the solution curve constant over time, i.e.

$$\frac{1}{-} \sum_{\substack{x_{j-1}(t) \\ x_{j-1}(t)}} u(x;t) dx = \text{constant.}$$
(2.8)

Di erentiation of (2.8) with respect to time yields

$$\frac{d}{dt} \int_{x_{j-1}(t)}^{z} \frac{1}{u(x;t)} dx = 0;$$
 (2.9)

which, since we are di erentiating under the integral sign we may utilise the Leibniz integral rule in order to obtain

$$0 = \frac{1}{2} - \frac{\sum_{x_j(t)} u(x;t) dx + 1}{\sum_{x_{j-1}(t)} u(x;t) dx + 1}$$

step. At j = N, ν is not actually de ned by (2.10) however we take $\nu_N = 0$.

2.4.2 Generation of New Meshes and Total Area

In order to generate the new mesh and total area under the solution curve to be used at the next time level we use a simple explicit Euler time stepping method.

Adaptive Time-Step 2.4.4

In order to allow our method to track the bahaviour of the solution appropriately we may use the scaling argument given in Budd et al. [3] to create a condition for varying the length of the time step. Budd et al. [3] state that Fisher's equation is invariant under the rescaling

$$(T \quad t) = (T \quad t); \tag{2.11}$$

$$u = \frac{1}{(p-1)}u; (2.12)$$

$$(T \quad t) = (T \quad t);$$
 (2.11)
 $u = \frac{1}{(p-1)}u;$ (2.12)
 $(x \quad x) = \frac{1}{2}(x \quad x);$ (2.13)

Nodes	i	t_0	Nodes		t_0	Nodes		t_0
11	1:71	10 ⁵	21	1	10 ⁵	41	1	10 ⁵
11	8 <i>:</i> 55	10 6	21	4 <i>:</i> 9	10 6	41	15	10 ⁶
11	4 <i>:</i> 275	10 ⁶	21	2 <i>:</i> 45	10 6	41	2 <i>:</i> 5	10 ⁶
11	2 <i>:</i> 1375	10 ⁶	21	1 <i>:</i> 225	10 6	41	1:24	10 ⁶

Table 2.1: Cases considered for the number of nodes in $x \ 2 \ [0;1]$ and t_0 in Fisher's equation

a nal time level closest to T. In this case t=1.225 10 6 is the smallest initial time step considered however it is not necessarily the case that a smaller

2.6 Can We Allow Moving Boundary Nodes?

Since we know that $v_N=0$ is chosen arbitrarily in order to x the boundary node and hence maintain the length of our domain, it may be of use to consider the possibility of allowing the boundary node to have a velocity other than $v_N=0$.

With this is in mind we investigate a possible solution to this problem which is to allow the boundary node to move with a certain velocity whilst maintaining its xed value of u = 0. This method has been applied to Fisher's equation here in order to examine what e ect this has on our solution when compared to those obtained in the previous sections where we had a xed boundary node.

In order to assign a velocity to the boundary node it is necessary to consider a di erent method to that laid out in Equation (2.10) since the value of u_j for the boundary node will be equal to zero and we may therefore not divide by it. To overcome this issue we consider a linear extrapolation of the velocities assigned to the two nearest nodes as shown in Figure (2.6), where the dotted line represents the linear extrapolation.



Figure 2.6: Demonstration of the method of linear extrapolation of velocities

We may express this linear extrapolation of the velocity using the expression

$$V_{J} = V_{J-1} + (X_{J} - X_{J-1}) \frac{(V_{J-1} - X_{J-2})}{(X_{J-1} - X_{J-2})};$$
 (2.16)

where the J subscript represents the boundary node.

The examples considered here are as laid out in Table (2.2) where t_0 represents the initial time step and all subsequent time steps are determined by Equation (2.15).

Nodes in <i>x</i> 2 [0;1]	11		21		41	
t_0	2 <i>:</i> 1375	10 ⁶	1:225	10 ⁶	1:24	10 ⁶

Table 2.2: Number of nodes and initial time steps used for comparison of xed and moving boundary node methods

A comparison of the results obtained using these two different methods are shown in Figure (2.7). Each of the lines in this gure represents the solution obtained at the nal time-step.

We also examine the difference in the maximum values of u obtained at the final time-step in order to look at the effect on our solution of allowing our boundary node to move. This is shown in Table (2.3) where the percentage refers to the percentage of the value of u_{MAX} obtained using a fixed boundary node method which can be achieved when using a moving boundary node method.

Nodes	Fixed Boundary Node	Moving Boundary Node	Percentage	
11	4664.85	7100.06	152.20%	
21	29144.84	3292.37	11.30%	
41	2933.36	1828.48	62.33%	

Table 2.3: Comparison of results obtained using a xed and a moving boundary node method

We can see from Figure (2.7) that allowing a method whereby the boundary node is allowed to move does not have a huge e ect in terms of the general shape of the solution which would suggest that there may be some potential in this method, however upon examination of Table (2.3) we see that there does not appear to be any reliable pattern in how close the two methods and time

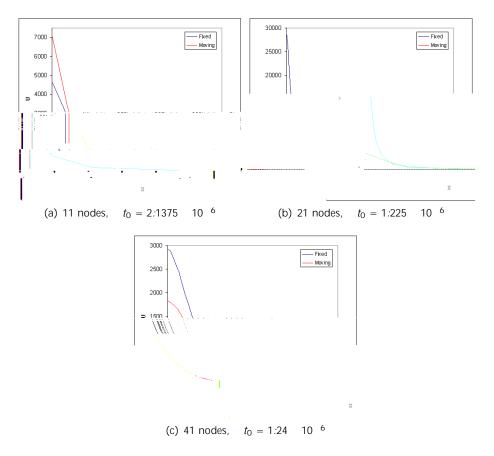


Figure 2.7: Comparison of results obtained using a xed and a moving boundary node method

solutions are associated with the number of nodes or the size of the time step.

The fact that this method of moving boundary nodes appears to be rather unpredictable in terms of how close to the xed boundary node solution the results we obtain are would suggest that this method should not be applied within the conservative moving mesh methods discussed here.

2.7 Method of Conservation for Fisher's Equation (with p = 3)

We now move on to considering the Fisher's equation with a dierent power, p, which in this case will be chosen as p = 3 which gives us Equation (2.3), i.e.

$$U_t = U_{XX} + U^3$$

Budd et al. [1] state that for Fisher's equation taking the form in Equation (2.1), we must conserve the quantity

and so in this case we conserve

$$Z u^2 dx: (2.17)$$

The method we will use in this section is exactly as laid out in Section (2.4) except for the fact that we will conserve the value in Equation (2.17) instead of the conserved value of

udx

which was conserved in the case where p=2. The cases which shall be considered here all use 41 nodes in $x \ge [0;1]$ and we utilise the t_0 values from the p=2 case of Fisher's equation.

2.8 Results for Fisher's equation (p = 3)

We begin by illustrating the behaviour of our solution as time passes. As mentioned previously, here we use 41 mesh points over the domain $x \ge [0;1]$ and we use the same initial time-steps, t_0 as weth.8[r thebyth.8[r the conthe fact that wep

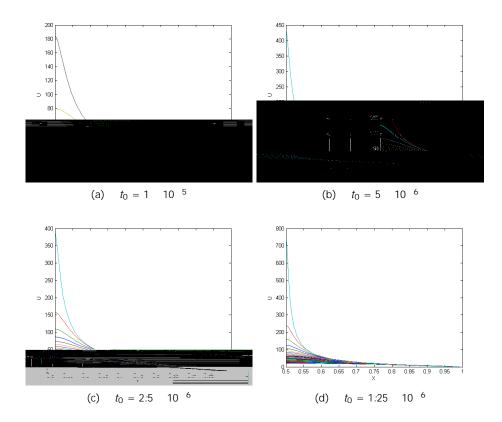


Figure 2.8: Solution of Fisher's equation (with p = 3) at the nal time step

As before we are able to see that the largest value of u that we are able to obtain is dependent on both the initial time-step and its development over time. We can also see that in this case (where p=3) we reach our largest solution in a much smaller number of time-steps than we were able to in the p=2 case. The reason for this is that the u^p term is the blow-up term, and in the case where p=3 this blow-up will occur faster due to the greater power of u.

We also examine the evolution of our mesh as time passes in order to see how the method works in terms of moving the mesh points in order to allow the resolution of the solution to be maintained.

Similar to the previous case we can see that as time passes, the nodes without a xed position move in towards the blow-up point. The main di erence between this case and the one considered previously is that it takes many fewer timesteps in order to reach the blow-up time, T. This can be seen by the fact that

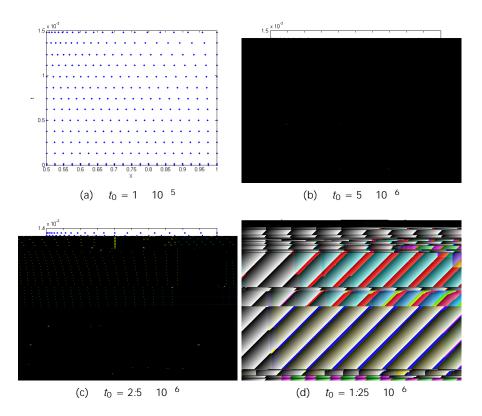


Figure 2.9: Mesh evolution in Fisher's equation with p=3

the time at which the mesh points really accelerate towards the blow-up point occurs much earlier than in the p=2 case.

Chapter 3

Alternative `Fisher Type' Equations

We now move the investigation into moving mesh methods on to look into their application for some further examples of `Fisher type' equations.

3.1 Introduction to `Fisher Type' Equations

According to Ockendon et al. [9], `Fisher type' equations are examples of semilinear reaction-di usion equations and they take the form

$$U_t = U_{xx} + f(U_t x_t t)$$
: (3.1)

Ockendon et al. [9] go on to state that these equations often appear in models of population dynamics, where the function f(u; x; t) can be either positive or negative depending upon the process which is being modelled.

The two examples of `Fisher type' equations which shall now be considered, in addition to those in Section (2

$$U_t = U_{XX} + U(1$$

`traditional' Fisher's equation.

The rst of these monitor functions given by Qiu and Sloan [10] is a standard arc-length monitor function. This takes the form

$$S = \frac{1}{M(x;t)} = 1 + \frac{2}{2} \frac{@u}{@x}; \qquad (3.4)$$

in which is a user-speci ed parameter that is given a value of = 2 in the paper by Qiu and Sloan [10]. Another monitor function considered in this same paper is that of a curvature monitor function of the form

$$M(x;t) = 1 + {}^{2} \frac{{}^{2}u}{{}^{2}x^{2}};$$
 (3.5)

where is again a user-speci ed parameter taking the value = 2 in the literature. Qiu and Sloan [10] then go on to de ne a modi ed monitor function which they believe captures the characteristics of the model e ectively and this is given in [10]. Another monitor function considered in this same paper is that of an extended curvature monitor function of the form

$$M(x;t) = 1 + {}^{2}(1 \quad u)^{2} + {}^{2}(a \quad u)^{2} \frac{e^{2}u}{e^{2}x^{2}}; \qquad (3.6)$$

and in this case we have three user-de ned parameters ; and a which are given the values = 1.5, = 0.1 and a = 1.015 in the paper by Qiu and Sloan [10].

In this investigation, we are concerned with implementing velocity-based moving mesh methods and with this in mind it will be the arc-length monitor function,

$$M(x;t) = 1 + \frac{2}{2} \frac{@u}{@x}^{2};$$

which shall be applied in subsequent sections. This is chosen as it should be suitable for use with both the 'traditional' Fisher's equation and the Cahn-Allen equation due to the fact that they share many similar characteristics.

3.3 `Traditional' Fisher's Equation

3.3.1 Problem Formation

During the investigation into the `traditional' Fisher's equation we shall consider the problem as laid out by Qiu and Sloan [10]. This gives the equation as

$$u_t = u_{xx} + u(1 \quad u); (3.7)$$

and shall be considered in the domain $x \ge [0;1]$.

It is also necessary to de ne both initial and boundary conditions in order to be able to solve this problem. The boundary conditions given in [10] are

$$\lim_{x!} u(x; t) = 1$$
 and $\lim_{x! \to t} u(x; t) = 0;$

and so we consider an approximate version of these which shall be b=x; t

initial condition as

$$u(x;0) = \begin{cases} 8 \\ \ge e^{-5x} & \text{for } 0 < x < 1 \\ \ge 0 & \text{for } x = 1 \end{cases}$$

3.4 Method for the `Traditional' Fisher's Equation

As discussed in Section (3.2), we create a velocity based method whereby an arc-length monitor function is used in order to guide the movement of the nodes. The method which shall be used for this problem is essentially a hybrid of two separate monitors since we use an area monitor to avoid a complicated inversion process which would be necessary were we to use an arc-length monitor in the retrieval of new approximations of the solution.

3.4.1 Generation of Nodal Velocities

We begin by splitting the domain x = 2 [0;1] into N equally sized intervals $(x_{j-1}(t); x_j(t))$, for j = 1; 2; ...; J. The arc-length of the solution curve for each of these intervals is given by

$$I_{j} = \sum_{\substack{x_{j-1}(t) \\ x_{j-1}(t)}} M dx;$$
 (3.8)

where
$$M = \bigcap_{X \to X} \overline{1 + u_X^2}$$
.

It is then possible to combine the arc-lengths for each of these intervals to give the arc-length of the entire domain, which shall be denoted . This gives

$$(t) = \int_{0}^{Z} M dx {3.9}$$

We may now di erentiate with respect to time in order to give the rate of change of the entire arc-length. This is given by

$$= \frac{d}{dt} \int_{0}^{Z_{1}} Mdx;$$
 (3.10)

to which we may apply the Leibniz integral rule to obtain

$$z = \int_{0}^{Z} \frac{\partial M}{\partial t} dx = \int_{0}^{Z} \frac{\partial u_{x} u_{tx}}{1 + u_{x}^{2}} dx$$

We are now able to substitute Equation (3.7) into this in order to obtain

$$\underline{z} = \int_{0}^{Z} \frac{1}{1 + u_{x}^{2}} \frac{u_{x}}{e_{x}} (u_{xx} + u(1 \quad u)) dx$$

In each interval we hold $u_x/\sqrt{1+u_x^2}$ constant and so we may take this outside of the integral to obtain

$$\int_{j=1}^{2} \frac{u_{x}}{1+u_{x}^{2}} u_{x_{j-\frac{1}{2}}(t)} [u_{xx}+u(1-u)]_{x_{j-1}(t)}^{x_{j}(t)}:$$

This may now be rearranged to give an expression for the nodal velocity which is given by

$$v_{j} = \frac{1}{M_{j}} - I_{j} - M_{j-1}v_{j-1} + [u_{xx} + u(1 - u)]_{X_{j-1}}^{X_{j}} - \frac{u_{x}}{M} x_{j-\frac{1}{2}}$$
:

3.4.2 New Mesh and Arc-Length Creation

In order to create the new meshes and total arc-length of the solution curve, we use a simple explicit Euler time stepping method.

This allows us to generate a new grid using the expression

$$X_i^{n+1} = X_i^n + t V_i^n$$

The same method is then used to generate a new arc-length for the entire domain which is given by

$$_{j}^{n+1}=\ _{j}^{n}+\ t_{-j}^{n}:$$

3.4.3 Recovery of New Approximations

We now resort to the use of the previous monitor function in order to obtain new approximations of the solution.

Firstly, we calculate the area under the solution curve for the entire domain, which shall be denoted by , and is given by

$$(t) = \int_{0}^{Z} u(x;t) dx$$

We now di erentiate with respect to time, which gives

$$- = \frac{d}{dt} \sum_{x_{j-1}}^{Z} u dx;$$

and we may now apply the Leibniz integral rule to this, which yields

$$- = \sum_{X_{j-1}}^{X_{j}} u_t dx + [uv]_{X_{j-1}}^{X_{j}}$$

Equation (3.8) may now be substituted into this to give

$$\begin{array}{rcl}
 & & Z_{x_{j}} \\
 & & (u_{xx} + u(1 & u))dx + [uv]_{x_{j-1}}^{x_{j}} \\
 & & Z_{x_{j}} \\
 & & = [u_{x}]_{x_{j-1}}^{x_{j}} + u(1 & u)dx + [uv]_{x_{j-1}}^{x_{j}}
\end{array}$$

It is now possible to obtain all of these values from previous stages of the method.

A simple explicit Euler time stepping method is used to generate a new total area under the solution curve which is given by

$$n+1 = n + t^{-n}$$
:

We then use this new value to give

$$Z_{x_{j+1}} udx = n+1;$$

to which we may apply the mid-point rule, giving

$$U_j^{n+1}[X_{j+1}^{n+1} \quad X_{j+1}^{n+1}] = {n+1};$$

and this may be rearranged to give an expression for the approximate solution which is

$$U_j^{n+1} = \frac{n+1}{\left[X_{j+1}^{n+1} \quad X_{j-1}^{n+1}\right]}$$

3.5 Cahn-Allen Equation

3.5.1 Problem Formation

Before we may investigate the application of a velocity based moving mesh method to the Cahn-Allen equation, we must begin by laying out the problem as it will be considered here. Lyons et al. [11] carry out numerical simulations of this equation which is given by

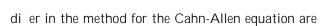
$$u_t = u_{xx} + u \quad u^3; (3.11)$$

and this shall be investigated on the domain $x \ge [-1;1]$.

It is also necessary to de ne both initial and boundary conditions for this problem. The boundary conditions given by Lyons et al. [11] are

$$u_x(1;t) = 0$$
 and $u_x(1;t) = 0;$

which hold at all time levels. We must now give an initial condition for consideration here, and this is again given by Lyons et al. [11] who give the initialsin83Ina626 ven. g 0 G [(])-3



$$(1 \quad \stackrel{?}{t}) \stackrel{x_j}{x}$$

$$= \frac{\times l}{j=1} \frac{u_X}{1 + u_X^2} \qquad u_{XX} + u(1 \quad u^2) \frac{x_j}{x_{j-1}} ;$$

$$- = [u_X]_{X_{j-1}}^{X_{j+1}} + \sum_{X_{j-1}}^{U_{j+1}} u(1 \quad u^2) dx + [uv]^{X_{j+1}}$$

X 1

u (´

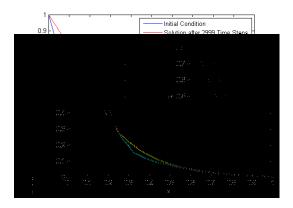


Figure 3.1: Solution obtained for the `Traditional' Fisher's equation

Figure (3.1) displays the result after 2999 time steps, which is the nal time step before we encounter an issue whereby nodes overtake one another. Upon examining this nal solution curve we can see that the curve appears to have formed the interface which we would expect to see according to Qiu and Sloan [10].

The next stage is to look at the evolution of the mesh over time, which is displayed in Figure (3.2).

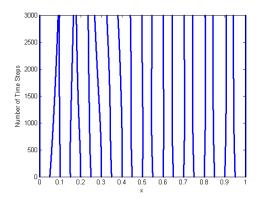


Figure 3.2: Mesh Evolution for the `Traditional' Fisher's equation

From Figure (3.2) we are able to see that in the left hand half of the domain, the nodes appear to be moving in towards the location at which the top of the interface forms. This is the behaviour we would wish to see when using this type of method as it would help to accurately resolve the solution at the ends

of the interface. Whilst there is a general pattern of nodal movement towards the desired location, the nodes move in at very dierent rates which may cause issues of nodal crossing before a nal solution has been obtained.

3.7.2 Results for the Cahn-Allen Equation

In Section (3.5.1), we explain that we shall use the domain $x \ge [-1;1]$ for our investigations into the Cahn-Allen equation. With this in mind we consider a mesh consisting of 41 nodes which initially have an equal spacing.

We begin by examining the results which were obtained for the solution curve, u. The results obtained after 99 and 199 time steps are displayed in Figure (3.3).

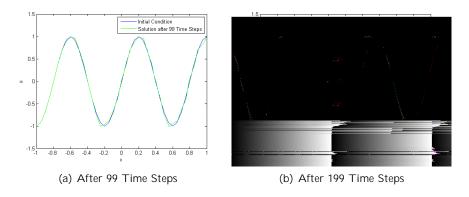


Figure 3.3: Solution obtained for the Cahn-Allen equation

We can see from Figure (3.3a) that after 99 time steps, the peaks and troughs in the solution curve appear to be moving towards eachother. Figure (3.3b) shows that after 199 time steps, the troughs of the solution curve appear to be developing some unphysical behaviour.

Next, we move on to examine the evolution of the mesh over the rst 199 time steps, and this is shown in Figure (3.4).

It is clear to see that across most of golutio1(o333(of)-333(n19-320(i1(ol33(of)c8(v)28(es167(toutep(curv)28(e

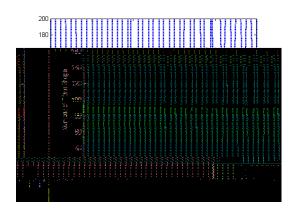


Figure 3.4: Mesh Evolution for the Cahn-Allen equation

the case with the `Traditional' Fisher's equation, the nodes move at very dierent rates leading to the problem of nodal overtaking which causes a breakdown of the solution. This nodal overtaking causes the solution after 199 time steps to display serious amounts of unphysical behaviour.

3.8 Summary of Other `Fisher Type' Equations

In this chapter we have laid out a method based on a hybrid of an arc-length monitor and an area monitor function.

When examining the application of this method to the `Traditional' Fisher's equation we obtained some positive results both in terms of the solution curve and the mesh evolution. We then applied the same method to the Cahn-Allen equation. From the results obtained we are able to demonstrate very limited potential in so much as there was nodal movement in the correct locations, however the breakdown of physical behaviour within a small number of time steps may suggest a need to seek a more appropriate method.

Chapter 4

The Nonlinear Schrodinger

as described in [12] and [13]. Budd et al. [12] and [13] state that this equation may be used to represent phenomena in both plasma physics and nonlinear optics.

As was the case with Fisher's equation, we may consider the NLS equation as a typical blow-up problem since, given suitable initial conditions, the solutions will display blow-up at a single blow-up point and this occurs within a nite blow-up time, *T*.

4.2 Problem Formation

In this investigation into the nonlinear Schrödinger equation we will consider the conservative form of the equation, and will look only at the case where d=2 since there is known to be an 'exact' solution for the d=1 case. This gives the NLS equation as

$$i\frac{\partial u}{\partial t} + \frac{1}{r}\frac{\partial}{\partial r} r\frac{\partial u}{\partial r} + juj^2 u = 0; \tag{4.3}$$

and it shall be considered on the domain $r \ge [0;1]$.

In order to solve this problem we must de ne both initial and boundary conditions. The boundary conditions considered for this particular problem are

$$u_r(0;t) = 0$$

$$u(1;t) = 0;$$

and we must choose an initial condition which satis es the boundary conditions whilst also being large enough to ensure blow-up will occur. With this in mind we choose an initial condition similar to that chosen for Fisher's equation however we will adapt it such that the part in the domain $x \ge [0.5;1]$ is stretched to cover the domain of $r \ge [0;1]$ used for the NLS equation. This gives our initial condition as

$$u(r;0) = 20 \sin \frac{1+r}{2}$$
 :

According to Budd et al. [12] there are two quantities which are invariant over time which are the `mass'

$$P = \int_{0}^{Z} \int u(r;t)j$$

Proof of Invariant Conserved Quantity

We begin our analytic investigation into the NLS equation by proving that the total integral of the quantity we aim to conserve will not vary over time. In other words we look to prove that

$$\frac{d}{dt} \int_{0}^{Z} uj^{2}rdr = 0;$$

where R is the end of the domain.

In order to prove that this is true we take the NLS equation as given in Equation (4.2), and into this we may substitute u = +i to obtain

$$i\frac{\mathscr{Q}}{\mathscr{Q}t}(+i)+\frac{1}{r}\frac{\mathscr{Q}}{\mathscr{Q}r}r\frac{\mathscr{Q}}{\mathscr{Q}r}(+i)+(^2+^2)(+i)=0;$$

which may be rearranged and split into its real and imaginary parts. This gives expressions for - and -, which are

$$- = \frac{@}{@t} = \frac{1}{r} \frac{@}{@r} r \frac{@}{@r} \qquad (^2 + ^2): \tag{4.4}$$

$$- = \frac{@}{@t} = \frac{1}{r} \frac{@}{@r} r \frac{@}{@r} + (^2 + ^2)$$
 (4.5)

We now look at the time derivative of our conserved quantity, which is given

by

$$\frac{d}{dt} \int_{0}^{Z_{R}} (^{2} + ^{2}) r dr; \qquad (4.6)$$

since $juj^2 = {}^2 + {}^2$, and this may be re-written as

It is now possible to substitute for - and - using Equations (4.4) and (4.5),

which gives

We may then simplify Equation (4.8) to leave

The next stage is to integrate each of the terms in Equation (4.9) by parts which will leave us with

$$2 r \stackrel{@}{=} r \qquad 2 \qquad \stackrel{@}{=} r r \stackrel{@}{=} dr \qquad 2 r \stackrel{@}{=} r \qquad + 2 \qquad \stackrel{@}{=} r r \stackrel{@}{=} dr; \qquad (4.10)$$

from which the integral terms cancel leaving us with

$$\frac{d}{dt} \int_{0}^{Z} (^{2} + ^{2})rdr = 2 r \frac{@}{@r} \int_{0}^{R} 2 r \frac{@}{@r} \int_{0}^{R}$$
(4.11)

$$= 2 (R) R^{\frac{@}{@r}} (R) \qquad 2 (0) 0^{\frac{@}{@r}} \qquad 2 (R) R^{\frac{@}{@r}} + 2 (0) 0^{\frac{@}{@r}};$$

which, using the boundary conditions $u_r(0;t)=0$ and u(1;t)=0 is equal to zero, and hence we have proven that

$$\frac{d}{dt} \int_{0}^{Z} \int uj^{2}r dr = \frac{d}{dt} \int_{0}^{Z} \left(2 + 2 \right) r dr = 0:$$

Derivation of Velocity Formula

In order to derive a formula for the velocity of the mesh nodes, we begin by considering the expression

$$Mv = \int_{0}^{Z} \frac{eM}{et} r dr;$$

which may be rearranged to give

$$V = \frac{1}{\left(\begin{array}{cc} 2 + 2 \end{array}\right)} \begin{bmatrix} Z & r_j \\ 0 & 2 & \frac{@}{@t} + 2 & \frac{@}{@t} \end{bmatrix} rdr:$$

We may then substitute for $\frac{@}{@t}$ and $\frac{@}{@t}$ using Equations (4.4) and (4.5), giving

$$V = \frac{1}{\binom{2+2}{r_j}} \begin{bmatrix} Z_{r_j} & Z_{e} & Z_{r_j} \\ Z_{r_j} & Z_{e} & dr + Z_{r_j} \\ Z_{r_j} & Z_{e} & Z_{r_j} \\ 0 & Z_{e} & dr & Z_{r_j} \end{bmatrix} = \begin{bmatrix} Z_{r_j} & Z_{r_j} & Z_{r_j} \\ Z_{r_j} & Z_{r_j} & dr \\ 0 & Z_{r_j} & Z_{r_j} & dr \end{bmatrix}$$

and this simpli es to

$$v = \frac{1}{\left(\begin{array}{ccc} 2 + 2 \end{array}\right)} \quad \begin{array}{cccc} Z & r_j \\ 0 & 2 & @r \\ \end{array} \quad r & \begin{array}{cccc} Q & P \\ \hline @r & \end{array} \quad dr \quad \begin{array}{cccc} Z & r_j \\ 0 & 2 & @r \\ \hline @r & \end{array} \quad r & \begin{array}{ccccc} Q & Q \\ \hline @r & \end{array} \quad dr \quad :$$

Now we may integrate by parts as in Section (4.3.1), which will give

$$V = \frac{1}{\left(\begin{array}{cc} 2 + 2 \end{array}\right)} 2r \frac{@}{@r} 2r \frac{@}{@r} : \tag{4.12}$$

The quotient rule applied to — will give

$$\frac{@}{@r} - = \frac{\frac{@}{@r} \frac{@}{@r}}{2}$$
 (4.13)

We are now able to substitute Equation (4.13) into Equation (4.12) to obtain

$$V = \frac{1}{\left(\begin{array}{cc} 2 + 2 \end{array}\right)} \quad 2r^{2} \frac{@}{@r} \quad - \quad {r_{j}}{?}$$

and the case where r = 0 returns only zero and so we now have an expression

for the nodal velocity which is

$$V = \frac{2r^{2}}{(2+2)} \frac{@}{@r} - \sum_{r_{j}} (4.14)$$

4.3.2 Calculating Conserved Quantities

In order to calculate the partial 'mass' values which we will hold constant, we begin by splitting our domain $r \ge [0;1]$ into N equally sized intervals with nodes denoted by $r_j(t)$ for j=0;1;...;J. As mentioned earlier, we aim to conserve the 'mass' in each interval which is given by

$$m_j = \frac{Z_{r_{j+1}(t)}}{r_{j-1}(t)} (^2 + ^2) r dr:$$
 (4.15)

4.3.3 Generation of New Meshes

The generation of a new mesh relies on us being able to de ne a suitable velocity for each node. Once this velocity is known, we may use a simple explicit Euler time stepping method.

An analytic derivation of the formula used to give the velocity of each node is laid out in Section (4.3.1) and the velocities of the nodes are given by

$$V_j = \frac{2r_j \frac{2}{j}}{\frac{2}{j} + \frac{2}{j}} \frac{@}{@r} \frac{j}{j} :$$

We then make the observation that

$$v_j = \frac{dr_j}{dt}$$
;

and this allows us to create a new grid using the standard explicit Euler time stepping method as given by the expression

$$r_j^{n+1} = r_j^n + t V_j;$$

where t represents the length of the time step. This new mesh may then be

used in the calculation of the values of and at the next time level.

4.3.4 Recovering New Approximations of and

New Approximations

In order to calculate a new approximation of the real part of our solution, $\,$, we begin by calculating

$$\int_{j}^{n} = \frac{Z_{r_{j+1}(t)}}{r_{j-1}(t)} r dr;$$
(4.16)

for each node. We then continue by examining how the value evolves over time and this is done by considering

$$-j^{n} = \frac{d}{dt} \sum_{\substack{r_{j+1}(t) \\ Z_{r_{j+1}(t)} \\ r_{j}}} rdr$$

$$= \sum_{\substack{r_{j+1}(t) \\ r_{j-1}(t)}} \underbrace{@}_{@t} rdr + [rv]_{r_{j-1}(t)}^{r_{j+1}(t)};$$

into which we may substitute Equation (4.4).

Once each of these values has been calculated for each node, we may then use a simple explicit Euler time stepping method to calculate a value of at the next time level using

$$j^{n+1} = j^n + t$$
 -

next time level using

part of our solution, , at the next time level and this is given by

$$_{j}^{n+1} = \frac{2 \int_{j}^{n+1} (r_{j+1}^{n+1})^{2} (r_{j+1}^{n+1})^{2}}{(r_{j+1}^{n+1})^{2}}$$
 (4.18)

New Approximations

We may now use a simple combination of Equations (4.15) and (4.18) to obtain an approximation for the imaginary part of the solution, . This begins by applying the mid-point rule to Equation (4.15) to give

$$m_{j} = \frac{Z r_{j+1}^{n+1}}{r_{j+1}^{n+1}} {2 + 2} r dr = {\binom{n+1}{j}}^{2} + {\binom{n+1}{j}}^{2} \frac{(r_{j+1}^{n+1})^{2} (r_{j+1}^{n+1})^{2}}{2};$$

which may be rearranged to obtain

This may be calculated since we may substitute Equation (4.18) in place of the 2 term. The value of m_j need not be recalculated at each time step since this quantity is time invariant as demonstrated analytically in Section (4.3.1).

This method may only be used to calculate values of and for j=1;...;J 1, meaning we have a requirement for an alternative method to calculate approximations at the nodes r_0 and r_J . For the values of and at r_J we use the boundary conditions to set

$$y = y = 0$$
:

The approximations at the node $r_0 = 0$ must be extrapolated from the values at the other nodes and the method used to do this is laid out in Section (4.3.6).

4.3.5 Lagrange Polynomial Exrapolation

Since we are unable to produce a solution value at the point r = 0 using the method laid out above it is necessary to utilise some other method to generate a

solution at r = 0. The method which is used here is that of Lagrange polynomial extrapolation whereby we create a polynomial which runs through a set of points and then we are able to use this to extend our solution curve to the point r = 0.

In this case we use the three points next to the point r=0 to create a quadratic polynomial which may be used to extend our solution curve.

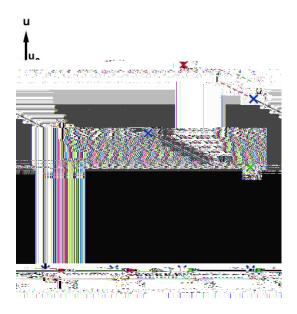


Figure 4.1: Demonstration of the method of Lagrange polynomials to extrapolate solutions

Figure (4.1) shows a simple example of this method, where the r_j are the radial coordinates and the u_j are the solution values. This example shows the case of a straight line solution however this method is equally valid when applied to curves such as those obtained in the solution of the NLS equation.

The formula which is used to create a quadratic running through the three points t49tthof4.isp vr

and this is applied at each time step to produce both a and value at the point r = 0.

This method yields some reasonable results however it is the case that this method will violate one of the boundary conditions. The reason for this is that our solution will not necessarily have the property that $u_r(0;t) = 0$, and this leads us to seek a method of extrapolation which will ensure we do not violate the boundary conditions.

4.3.6 Improved Polynomial Exrapolation

In order to ensure we do not violate the boundary condition $u_r(0;t) = 0$, we begin by creating a quadratic polynomial of the form

$$u_j = ar_i^2 + br_j + c$$

and then use the solutions and the radial coordinates at two other points in order to specify the values of each coe cient.

Using the boundary condition $u_r(0;t) = 0$ gives

$$\frac{du_j}{dr_j} = 2ar_j + b = 0;$$

from which we may deduce that b = 0 leaving our quadratic polynomial as

$$u_j = ar_j^2 + c$$
:

We now use the two closest values of u and r to assign values to the other coe cients which will be given by

$$a = \frac{u_1}{r_1^2} \frac{u_2}{r_2^2}$$

and

$$c = u_2 \quad ar_2^2$$
:

This now gives us a polynomial of the form given above which may be used to calculate the solution value at the point r = 0, and using this method clearly ensures that our solution will satisfy the boundary condition $u_r(0;t) = 0$ which takes e ect at the point r = 0.

4.4 Results for Mass Conservative Method for Nonlinear Schredinger Equation

In order to examine the results obtained for the above method whereby a mass monitor function was used, we begin by showing how the real and imaginary parts of the solution develop over time and then look at the evolution of the mesh over the same time period.

The example considered here uses a time step of t=1 10 6, a mesh consisting of 11 nodes with an initial spacing of r=0.1 and uses the initial condition $u(r;0)=20\sin$

most certainly not consistent with what we would expect to see from a blow-up problem.

The results which were obtained for the imaginary part of the solution are shown in Figure (4.3).

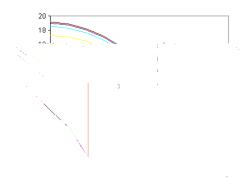


Figure 4.3: Imaginary part of the `mass' conservative solution of the Nonlinear Schrodinger Equation

We can clearly see from Figure (4.3) that this method will result in the imaginary part of the solution, , will increase over time. This does not necessarily go against what we should expect to see from a known blow-up problem.

We also examine the evolution of the mesh over time, and this is shown in Figure (4.4).

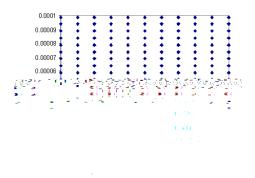


Figure 4.4: Mesh Evolution of the `mass' conservative solution of the Nonlinear Schrødinger Equation

From Figure (4.4) we are able to see that the method laid out in the previous

sections will cause the nodes to move very slightly. This change is however likely to be too small to give much bene t in terms of accurate representation of the solutions obtained.

Consideration of all of the results obtained together would suggest that this method does not suitably model the behaviour which should be produced from the NLS equation. The most likely reason for the failure of this method is that whilst the `mass' conservation property is necessary, it is not su cient to capture the correct behaviour of our solution.

4.5 Area Conservative Method for Non-linear Schredinger Equation

We now consider a velocity-based method whereby the velocity assigned to each node in order to ensure that the area under the solution curve held in each interval remains constant over time.

As explained previously, solutions of the NLS equation consist of a real part, and an imaginary part, . With this in mind we de ne two separate meshes. One of these is for use in calculating solutions and the other for the solutions and these shall be denoted r and r respectively.

the solution for each interval as given by

$$a_{j} = \sum_{\substack{r_{j-1}(t) \\ r_{j-1}(t)}} (r; t) r dr;$$
 (4.19)

The next step is to sum the a_j value from each interval to give the area under the solution curve for the entire domain, . This is given by

$$(t) = \begin{cases} Z_{1} \\ (r;t)rdr \end{cases}$$
 (4.20)

Di erentiation of Equation (4.20) with respect to time gives

$$-(t) = \frac{d}{dt} \int_{0}^{z} r dr = \int_{0}^{z} r dr$$

use the Leibniz integral rule to obtain

$$0 = -\frac{1}{2} - \frac{Z_{r_{j}(t)}}{r_{j-1}(t)} (r;t)rdr + \frac{1}{2} \frac{Z_{r_{j}(t)}}{e^{t}} \frac{e^{t}}{e^{t}} rdr + [rv]_{r_{j-1}(t)}^{r_{j}(t)} :$$

Using Equations (4.5) and (4.19), allows us to re-write this as

$$0 = -a_{j} + r \frac{@}{@r} + r_{j-1} + r_{j-1}$$

where ν represents the velocity of the mesh used in calculations. Finally, rearranging this will gi -1.494 Td [()]TJ/F8 9.9626 Tf 10.097 1.494 Td [(represen)28(ts)-410(the)-4.738yhan.

4.5.2 Generating New Meshes and Total Areas

and the mid-point rule my be applied to this in order to obtain

$$\frac{1}{(t)} _{j}(t) \frac{r_{j+1}^{2}(t) _{j} r_{j-1}^{2}(t)}{2} = \frac{1}{(0)} _{j}(0) \frac{r_{j+1}^{2}(0) _{j} r_{j-1}^{2}(0)}{2} :$$

This may be rearranged to obtain

$$j(t) = j(0) \frac{(t) r_{j+1}^2(0) r_{j-1}^2(0)}{(0) r_{j+1}^2(t) r_{j-1}^2(t)};$$

and this is used to recover a new approximation of the imaginary part of the solution.

Utilising the same method applied to

$$\frac{1}{r_{j-1}(t)}^{\sum_{r_{j+1}(t)} (r;t)rdr;}$$

will give the expression used to recover the real part of the solution which is

$$j(t) = j(0) \frac{(t) r_{j+1}^2(0) r_{j-1}^2(0)}{(0) r_{j+1}^2(t) r_{j-1}^2(t)}:$$

4.6 Results for the Area Conservation Method for the Nonlinear Schredinger Equation

In examining the results obtained for the area conservative method applied to the NLS equation, we begin by looking at the velocities of the nodes in both the and meshes. Based on the theory of this type of problem we should condition of the form

$$6^{p} = \frac{1}{2}e^{-r^{2}}$$

which is considered on the domain $r \ge [0/5]$. The nodal velocities obtained for the rst time step are shown in Figure (4.5).

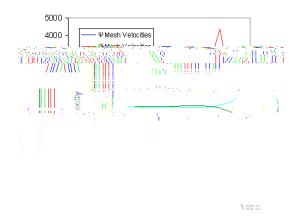


Figure 4.5: Nodal velocities obtained for the NLS equation with an initial condition of 6 $\overline{2}e^{-r^2}$

Figure (4.5) clearly shows that some of the nodes in each mesh will have a velocity such that they move to the left and some will have velocities such that they move to the right. Movements of this type will obviously not aid in accurately resolving the detail of the blow-up in the solution as time passes.

Another initial condition was considered in order to test whether the unusual velocities obtained for the other initial condition were some type of anomaly. The condition that was next to be considered was of the form

$$20\sin \frac{1+r}{2}$$

and this was considered on the domain $r \ge [0;1]$. As before we present a plot of the nodal velocities obtained for the rst time step of this method in Figure (4.6).

We are clearly able to see that, as was the case for the other initial condition, some of the nodes will move to the left and some will move to the right.

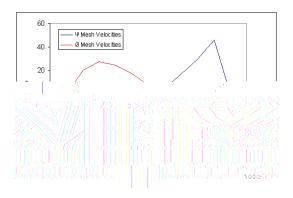


Figure 4.6: Nodal velocities obtained for the NLS equation with an initial condition of 20 sin $\frac{1+r}{2}$

Again, we are able to say that mesh evolution of this form will not be of use in attempting to aid the resolution of the blow-up in the solution of the NLS equation.

The consideration of both of these initial conditions and the velocities obtained for the nodes within each mesh, allows us to conclude that this method is not suitable for use in the solution of the NLS equation.

4.7 Nonlinear Schredinger Equation Summary

Within this chapter there has been two methods set out to solve the NLS equation on a moving mesh.

The rst method was based on the use of a 'mass' monitor function and this resulted in a mesh which did not evolve in a suitable manner to help resolve the blow-up that our solution should exhibit.

We then went on to consider a method based around the use of an area monitor function. This method did create a mesh within which the nodes moved, however the direction of nodal movements was not in a manner which we may deem as being suitable for helping to resolve the blow-up in the solution of the NLS equation.

Chapter 5

Discussion of Project

5.1 Summary

In this dissertation we have carried out an investigation into the application of velocity-based moving mesh methods based on various monitor functions. The methods investigated in this project were applied to a number of semi-linear time dependant partial di erential equations.

Chapter 1 began by explaining the motivation for this investigation into velocity-based moving mesh methods as well as the types of problems to which these methods were applied. In Chapter 2 we demonstrated the e ectiveness of a method based upon an area conservation monitor function for two di erent powers of blow-up term. Some other `Fisher type' equations, namely the `traditional' Fisher's equation and the Cahn-Allen equation were investigated in Chapter 3. The method applied to these equations was built upon a hybrid of an arc-length monitor function and an area monitor function. Finally, Chapter

5.2 Conclusions

Throughout this dissertation we have outlined a number of di erent methods which have been applied to a variety of semi-linear PDEs and have achieved varying degrees of success.

The method which was applied to Fisher's equation, which was based on an area monitor function generated very positive results. This chapter demonstrated the ability of the method to produce results with a good level of resolution in the blow-up of the solution whilst using a small number of nodes. It is clear from the results obtained that using an area monitor function allowed the mesh to e ectively cluster nodes around the blow-up point.

A method based upon a hybrid of an arc-length monitor function and an area

In general it is clear from the work carried out in this dissertation that these velocity-based moving mesh methods have some potential in terms of reallocating nodes in such a way that the resolution in certain areas of the solution is increased. This also aids with the e-ciency of the numerical methods used to solve these problems since we may accurately represent the solution with fewer nodes than would be necessary when using a standard xed mesh method. It is also clear that the choice of an appropriate monitor function is essential for these methods to be successful. The nal conclusion to draw from this dissertation is that whilst we have demonstrated the potential of velocity-based moving mesh methods, they are not always successful and as such they should

ered. There are two main ways in which we may seek to improve our method's e ciency. Firstly, we may look at the numerical code used to obtain the results in order to ensure it holds a minimum amount of information at any time. We may also wish to ensure that all calculations are carried out using the smallest number of operations possible. The other way in which the computational e ciency of our method may be improved would be to look into alternative time stepping techniques. This could potentially allow us to use fewer time steps in order to reach our nal solution and this could signi cantly reduce the amount of operations necessary to obtain nal results.

The investigation into the `traditional' Fisher's and Cahn-Allen equations

Bibliography

[1] C. Budd, W. Huang, and R. Russell, \Adaptivity with moving grids," *Acta Numerica*, 2009.

[2]

- [9] J. Ockendon, S. Howison, A. Lacey, and A. Movchan, *Applied partial dif- ferential equations*. Oxford University Press, 1999.
- [10] Y. Qiu and D. Sloan, \Numerical solution of sher's equation using a moving mesh method," *Journal of Computational Physics*, 1998.
- [11] W. Lyons, H. Ceniceros, S. Chandresekaran, and M. Gu, \Fast algorithms for spectral collocation with non-periodic boundary conditions," *Journal of Computational Physics*, 2004.
- [12] C. Budd, S. Chen, and R. Russell, \New self-similar solutions of the non-linear schriy1Journal